61. Angular Distortions at Tetracoordinate Carbon

Planoid Configurations in Substituted Spiro[4.4]nonanes

by **Wolfgang Luef**[a]), **Reinhart Keese**[a])*, and **Hans-Beat Bürgi**[b])

[a]) Institut für organische Chemie der Universität
[b]) Laboratorium für chemische und mineralogische Kristallographie, Freiestrasse 3, CH-3012 Bern

Dedicated to Professor *Albert Eschenmoser*

(24. II. 87)

The configuration of the spiro centre in polycyclic compounds containing a spiro[4.4]nonane substructure is analyzed in terms of symmetry coordinates. As revealed by X-ray structures of such compounds, the local distortions around the quaternary C-atom are dominated by a decrease of the ring-bond angles at the spiro centre and a twist of one ring relative to the other. The planoid deformations given by the planarization index P_C are comparatively small for spiro[4.4]nonanes, which contain either no additional bridges between the rings or only α,β'- or β,β'-polymethylene bridges. This indicates that the local strain in the spiro $C(C)_4$ fragments is rather small.

The theory of *van't Hoff* [1] and *Le Bel* [2] requires the four ligands of a saturated C-atom to have tetrahedral geometry [3]. A regular tetrahedral structure is not implied, and indeed, only few molecules contain a tetracoordinate C-atom with exact T or T_d symmetry. Distortions from regular tetrahedral coordination have been investigated ever since *v. Baeyer* first discussed bond-angle deformations in small carbocyclic ring systems and correlated them with strain energy [4].

A survey of polycyclic molecules [5] shows that bond-angle distortions at tertiary or quaternary C-atoms are often associated with local C_{3v} symmetry as in cubane [6], dodecahedrane [7], and the propellanes; an extreme example of this kind is [1.1.1]propellane, where strain is related to two inverted C-atoms [8].

Strained molecules containing quaternary C-atoms with local fourfold rotation-inversion (D_{2d}) or orthorhombic (D_2) symmetry have been much less investigated. Examples are the spiro hydrocarbons and the fenestranes (which may be considered as bridged spiro compounds[1])). The deformations from local T_d symmetry in the bond angles of these molecules indicate a tendency towards planar tetracoordinate C-atoms. In spiropentane the two ring-bond angles at the spiro centre decrease, whereas the other four angles increase. In the fenestranes on the other hand, the four ring angles decrease and the remaining two angles increase. To assess the type and extent of deformation, the angles are analyzed in terms of symmetry-deformation coordinates. On the basis of these coordinates, a simple measure of the degree of planarization of tetracoordinate C-atoms, *i.e.* of their planoid deformation, may be defined.

[1]) Paddlanes [9] and pyramidanes also belong to the class of strained hydrocarbons with local geometry of twofold and fourfold symmetry, respectively [5].

In this paper, we discuss distortions at the spiro centre of spiro[4.4]nonanes that show no C chains between the α- and α′-positions. The analysis concentrates on structural data obtained by X-ray diffraction. In [10], spiro[4.4]nonanes with bridges between the α- and α′-positions, including the [5.5.5.5]fenestranes are analyzed. All these compounds may be considered a subclass of the centropolycyclics, as defined by *Gund* and *Gund* [11].

Symmetry Coordinates. – The use of these coordinates for analyzing static distortions of MX_4 structures from T_d symmetry has been elaborated by *Murray-Rust et al.* [12]. Symmetry coordinates are linear combinations of bond lengths or angles that transform as irreducible representations of the symmetry group of a reference structure *(Appendix 1)*. In our case, the reference has T_d symmetry and may be identified with the C skeleton of neopentane. The total distortion in a $C(C)_4$ fragment is expressed by the total displacement vector $\boldsymbol{s}$ with components s_j along the symmetry coordinates S_j, *i.e.* $\boldsymbol{s} = s_j S_j$ with length $|\boldsymbol{s}| = (\Sigma_j s_j^2)^{1/2}$.

A subset of symmetry displacements will be relevant if only a part of the total distortion is of interest, or if a distorted $C(C)_4$ fragment preserves certain symmetry elements.

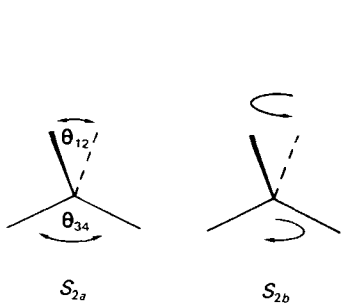

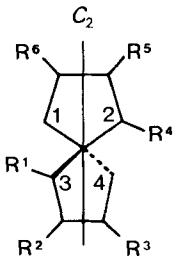

1

Fig. 1. *Compression* ($S_{2a}(E)$) *and twist deformation* ($S_{2b}(E)$) *of the* $C(C)_4$ *fragment of* **1**

$R^1 + R^6 = -(CH_2)_m-$
$R^2 + R^6 = -(CH_2)_n-$
$R^3 + R^4 = -(CH_2)_o-$
$R^3 + R^5 = -(CH_2)_p-$
$m, n, o, p = 0, 3–7$

In this paper, the primary interest is in angle deformations which lead to planar $C(C)_4$ fragments. Only two symmetry coordinates are relevant: the degenerate pair $S_{2a}(E)$ and $S_{2b}(E)$. The former describes angle opening or closing of a pair of opposite angles at the expense of the other four and will be referred to as 'compression' *(Fig. 1)*. Fragments deformed along S_{2a} retain D_{2d} symmetry. In the limit, this deformation leads to a square planar ($s_{2a} > 0$) or linear fragment ($s_{2a} < 0$). S_{2b} describes a deformation in which one pair of opposite angles remains invariant, a second pair opens up, and the third pair closes by an appropriate amount (see *Appendix 1*). It may be pictured as a rotation of one $C(C)_2$ fragment with respect to the other and will be referred to as 'twist' deformation. The deformed fragment retains D_2 symmetry and in the limit becomes rectangular planar[2]).

[2]) Angle deformations $S_{4a}(T_2)$, $S_{4b}(T_2)$, $S_{4c}(T_2)$ belonging to the irreducible representation T_2 lead to fragments preserving C_1, C_{3v} and C_{2v} of C_s symmetry, respectively.

The degree of deformation is $s_2 = (s_{2a}^2 + s_{2b}^2)^{1/2}$. The (hypothetical) fragment structure with all deformations removed except for the planarizing deformation S_{2a} and S_{2b} is obtained by averaging the three pairs of opposite bond angles [12a].

There is a complication: given a distorted fragment, labels 1 through 4 can be assigned to the four C ligands in 24 different ways, leading, in general, to six distortion vectors with different components s_{2a} and s_{2b}, but with identical length s_2. The six vectors form angles of $\pm\,\alpha$, $120° \pm \alpha$, and $240° \pm \alpha$ with the coordinate axis S_{2a}, *i.e.* their distribution over the S_{2a}, S_{2b} plane shows *3m* symmetry *(Fig. 2)*[3]). There is always a labeling for which $0 < \alpha < 60°$ and, therefore, $s_{2a}/s_{2b} \geq 1/\sqrt{3}$. For deformation vectors along S_{2a} with components $s_{2a} \neq 0$ and $s_{2b} = 0$, α equals 0°; the deformation corresponds to opening θ_{12} and θ_{34} while closing the other four. Vectors with components $s_{2a} = s_{2b}/\sqrt{3}$, point along $-S''_{2a}$, and α equals 60° *(Fig. 2)*; the deformation corresponds to closing θ_{14} and θ_{23} while opening the other four. In either case, the fragment retains D_{2d} symmetry. The D_4 axis

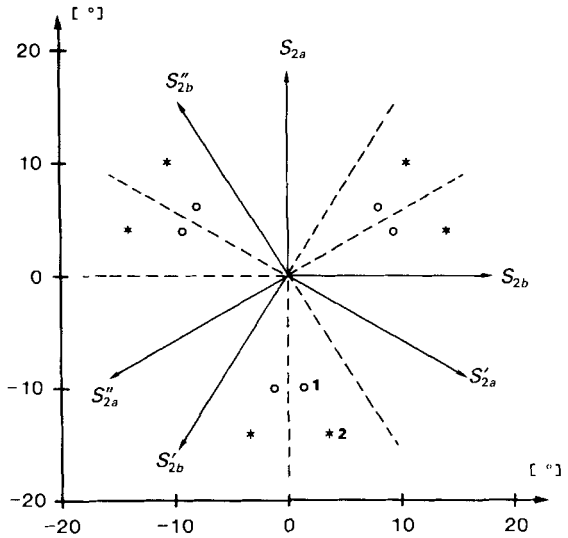

Fig. 2. s_{2a}(E) vs. s_{2b}(E) *bond-angle deformation vectors for molecules* **1** (○) *and* **2** (*) *in relation to the three sets of* S_{2a}/S_{2b} *coordinates*

bisects θ_{12} and θ_{23} in the former, θ_{14} and θ_{23} in the latter case. Another special case is $\alpha = 30°$, corresponding to a deformation along $-S'_{2b}$ *(Fig. 2)*. It may be looked at as pure twist deformation about the axis bisecting θ_{13} and θ_{24} or, alternatively, as a combination of compression and twist with respect to the axis bisecting θ_{12} and θ_{34} (with the condition that $s_{2a} = \sqrt{3}s_{2b}$). For all deformations with $0 < \alpha < 60°$, the fragment retains D_2 symmetry.

Index of Planarization P_C. – Since, in the limit, two symmetry coordinates lead to planar $C(C)_4$ fragments, the question arises, whether the degree of planarization can be expressed in terms of a single quantity. This is indeed possible as may be seen from the following argument: the geometrically accessible asymmetric unit in the S_{2a},S_{2b} plane is a

[3]) Only the endpoints of the vectors are indicated.

right angled triangle with corners (0,0), (103,92°, 0°), and (103.92°, 180°). Moving from the first point to the second corresponds to distorting a regular tetrahedral into a square-planar fragment. Moving from the second to the third corresponds to changing a square-planar into a rectangular-planar and ultimately into a linear fragment without changing planarity. This argument may be generalized for any line $0 \leqslant s_{2a} \leqslant 103.92°$ (with the side condition that $s_{2a} > s_{2b}/\sqrt{3}$). Thus, s_{2a} is a measure of planarization; an alternative measure is the planarization index $P_C = s_{2a}/s_{2a}(\max)$ which is in the range from 0 to 1[4]). P_C is proportional to $s_{2a}(\max) - 1/4\sum_i^4 \sin^{-1}(\Delta x_i/r_o)$, where Δx_i is the deviation of substituent i from the best plane through the fragment.

Spiro[4.4]nonanes. – In spiro compounds of type **I** *(Fig. 1)*, all deformations will be related to the C_2 axis bisecting the two rings. This reduces the number of possibilities for assigning labels to the four ligands of the spiro center to eight and the distortion vectors with different components s_{2a} and s_{2b} – but with identical length s_2 – to two. This is reduced to a single possibility, if it is required that the twist deformation $s_{2b} > 0$. Deformations along S_{2a} with $s_{2a} > 0$ correspond to opening the intra-ring bond angles θ_{12} and θ_{34}, whereas $s_{2a} < 0$ corresponds to closing the intra-ring bond angles θ_{12} and θ_{34}. In this latter case, the deformation vector may not follow the side condition $s_{2a} \geqslant s_{2b}/\sqrt{3}$ implicit in the definition of P_C. If $s_{2a} < 0$, it may be shown that $P_C = (-s_{2a} + \sqrt{3}\, s_{2b})/2s_{2a}(\max)$.

Examples **1** *and* **2**. As an illustration of the above, the spiro structures **1** [15] and **2** [16] are analyzed. The two differ only in their peripheral substituents. Results of the crystal-structure analysis of **1** and **2** are summarized in the *Table*.

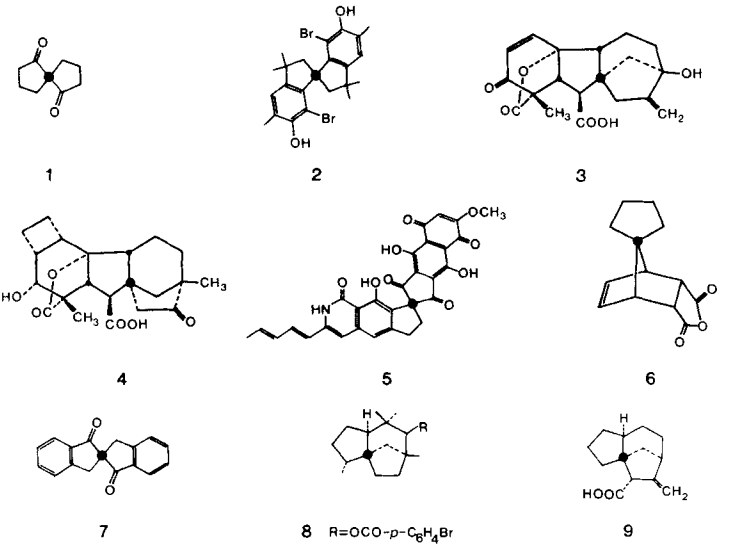

[4]) Analogously, a linearization index $L_C = s_{2b}/s_{2b}(\max)$ may be defined (with the side condition $0 \leqslant s_{2b} \leqslant \sqrt{3}\, s_{2a}$). L_C is proportional to $s_{2b}(\max) - 1/4\sum_i^4 \sin^{-1}(\Delta y_i/r_o)$, where Δy_i is the deviation of substituent i from the best line through the fragment (r_o is the C–C bond distance). $L_C = 1$ implies that pairs of substituents occupy the same position (*e.g.* corresponding to a linear MgCMg fragment). An approximate upper limit on L_C, which is chemically feasible in the context of $C(C)_4$ fragments, may be estimated from the bond angles for spiropentadiene [13] calculated with the MNDO method [14] (D_{2d}, $\theta_{12} = 53.2°$, $\theta_{13} = 143°$). Here $L_C \approx 0.5$ and $P_C \approx 0.5$.

Table. *Bond-Angle Deformation Vectors* [°] *for the Spiro Centre in* **1** [15] *and* **2** [16]

	1	**2**
$s_{2a}(E)$	–9.988	–14.145
$s_{2b}(E)$	1.300	3.500
$s_{4a}(T_2)$	0.0	0.707
$s_{4b}(T_2)$	–1.556	2.121
$s_{4c}(T_2)$	0.0	0.0
$s_2(E)$	10.072	14.572
$s_4(T_2)$	1.556	2.236
α	172.58	166.1

In both cases, the two dimensional $s_2(E)$ displacement vector is longer than $s_4(T_2)$; the length $s_2(E)$ and the difference $s_2 - s_4$ increase from **1** to **2**. In **1**, the angle $\alpha = 172.6°$, *i.e.* the distortion is mainly compression ($\alpha = 180°$; *cf. Fig. 4*). There is no significant twist, and the approximate symmetry is D_{2d}. In **2**, $\alpha = 166.1°$, slightly smaller than in **1**. This indicates, that twist contributes more to the overall bond-angle deformation.

Data Selection. The *Cambridge Structural Data Base* (updated version of June 1985 with 42 145 entries [17]) was searched for structures containing spiro[4.4]nonane substructures which contain no additional bridges between the rings or only α,β'- or β,β'-polymethylene bridges. From the 57 entries found, those with $R > 0.1$ and σ_{av} (C–C) > 0.03 Å in the central $C(C)_4$ fragment of each structure were rejected. From the remaining 36 structures containing 36 spiro[4.4]nonane subunits, bond angles and bond lengths were taken, as reported. The molecules analyzed are specified by their *CAS*-registry number, reference code, formula number (if applicable), and by their symmetry deformation vectors s_{2a}, s_{2b}, and $s_4(T_2)$ *(Appendix 2)*.

Discussion. The distortions at the spiro centre are first analyzed with respect to $S_2(E)$ and $S_4(T_2)$ deformations *(Fig. 3)*[3]).

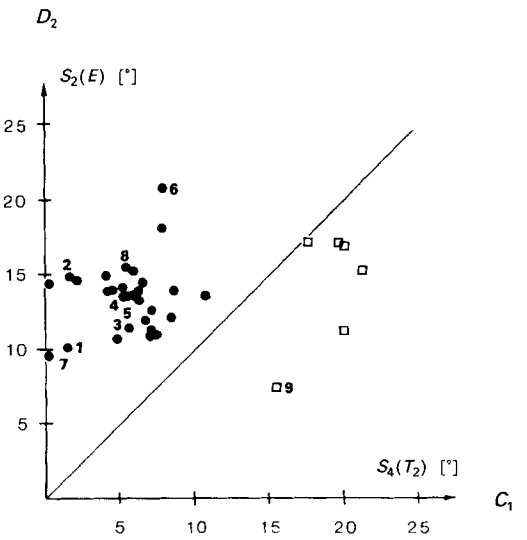

Fig. 3. *Bond-angle distortion vectors* $s_2(E)$ vs. $s_4(T_2)$ [°] *for the spiro* $C(C)_4$ *fragment in substituted spiro[4.4]-nonanes of type* **I** (*Fig. 1*). ●: Structures with $s_2(E) > s_4(T_2)$, □: structures with $s_2(E) < s_4(T_2)$.

The $s_2(E)$ bond-angle deformation vectors are – apart from a few exceptions – larger than the $s_4(T_2)$ vectors[5]). This indicates that the molecular constraints in these spiro compounds lead to structures where compression and twist dominate over $S_4(T_2)$-type deformations. *Figs. 3* and *4* show that most s_2 values are in the range of 10°–20°; the calculated planarization indices P_C are generally smaller than 0.2. Bond-angle deformations of essentially pure $S_2(E)$ character are very rare in the bridged spiro[4.4]nonanes investigated. The contribution for most of the spiro molecules considered is partly due to the substituents, which affect opposite bond angles to an unequal extent.

Examples of structures with dominating $S_2(E)$ distortions occur in natural products like the gibberillines **3** ($s_2(E) = 11.39°$, $s_4(T_2) = 5.67°$), **4** ($s_2(E) = 13.50°$, $s_4(T_2) = 5.53°$) and the antibioticum fredericamycin **5** as well as in synthetic molecules like the spiro compounds **6**, **7** ($s_2(E) = 9.73°$, $s_4(T_2) = 0.187°$), and **8**. Comparison of the spiro fragments in **1**, **2**, **5**, and **7** leads to some simple relationships between substitution and twist distortion. $S_2(E)$ Distortions in **1** and **7** are rather similar, indicating that annellation by Ph rings in the β,γ-position does not alter the configuration at the spiro centre. The difference between the $s_2(E)$ vectors in **1** and **2** can be attributed to the different substitution patterns in the spiro rings. Whereas **1** contains a C=O group adjacent to the quaternary C-atom in each of the rings, **2** contains a double bond (part of an annellated

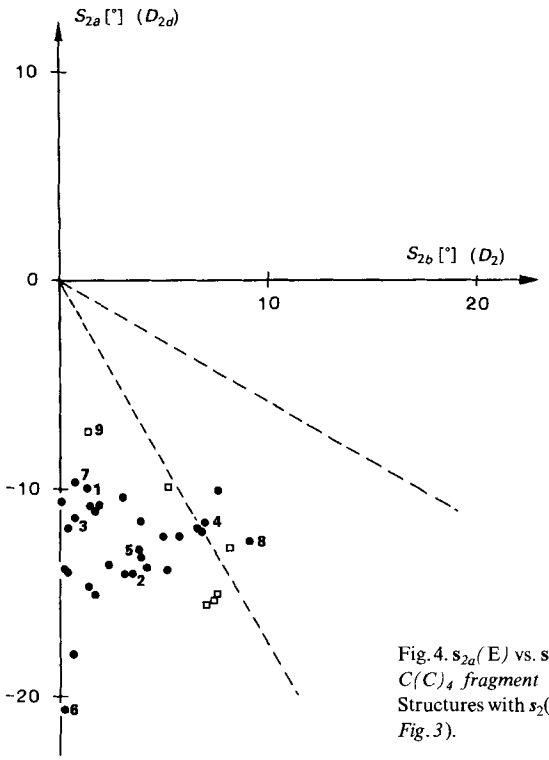

Fig. 4. $s_{2a}(E)$ vs. $s_{2b}(E)$ *bond-angle deformation vectors for the spiro* $C(C)_4$ *fragment in substituted spiro[4.4]nonanes of type* **1**. ●: Structures with $s_2(E) > s_4(T_2)$, □: structures with $s_2(E) < s_4(T_2)$ (*cf. Fig. 3*).

[5]) The deformation vectors for spiro C-atoms bonded to saturated groups are not distinguished from those C-atoms bonded to unsaturated groups.

aromatic ring) and geminal CH_3 groups in both rings. The increase in $s_2(E)$ is due to larger contributions from both compression (s_{2a}) and twist (s_{2b}) to the overall planoid deformation (*Fig. 4*)[3]). In fredericamycin **5**, the substitution pattern in one spiro ring resembles **2**, that in the other resembles **7**. Whereas $s_4(T_2)$ equals 2.24° in **2** and 0.19° in **7**, it is 5.38° in **5**; s_{2a} and s_{2b} are closely similar for **2** and **5**, but not for **5** and **7** (*Fig. 4* and *Appendix 2*).

Similar substituent effects are apparent from a comparison of the tricyclic compounds **8** and **9**, which contain the same framework substituted differently. Whereas in structure **8** $s_2(E)$ dominates over $s_4(T_2)$ (15.44° *vs.* 5.45°), in **9** $s_4(T_2)$ is larger than $s_2(E)$ (15.5° *vs.* 7.37°). Since $s_4(T_2)$ deformations are of minor importance in the context of planoid deformations, a more detailed analysis of the structural features has not been pursued for the few molecules in which $s_4(T_2) > s_2(E)$.

The $s_2(E)$ bond-angle deformation vectors of the molecules with $s_2(E) > s_4(T_2)$ have been analyzed with respect to their compression (s_{2a}) and twist (s_{2b}) components (*Fig. 4*)[3]). A wide range of bond-angle distortions is apparent, but they cluster between $\alpha = 150°$ and $\alpha = 180°$. Characteristic of the local spiro structure in these molecules are twist deformations and decreased intra-ring bond angles. Examples of quaternary C-atoms showing considerable compression ($|s_{2a}| \gg s_{2b}$; *Fig. 4*) are given by the polycyclic molecules **3** and **6**.

Comparison of the gibberellines **3** and **4** reveals a further structural difference: the spiro centre in **3** is characterized by $s_{2a}(E) = -11.37°$ and $s_{2b}(E) = 0.70°$, whereas in **4** $s_{2a}(E) = -11.58°$ and $s_{2b}(E) = 6.95°$. The configurational change in one of the bridges between the two spiro rings and in the substitution pattern apparently leads to a significant change in the twist (s_{2b}) deformation.

Bond-Angle *vs.* Bond-Distance Deformations. – It is apparent from *Fig. 5a* that no significant correlation exists between the planarizing bond-angle distortions $s_{2a}(E)$ and

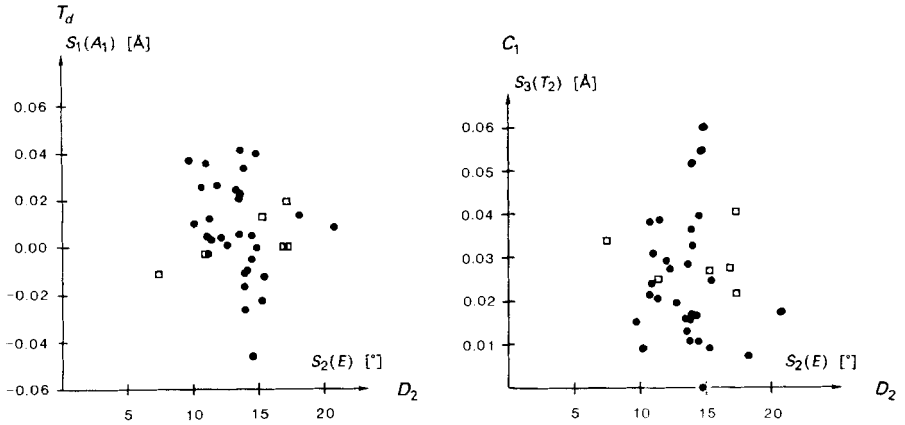

Fig. 5. *Bond-length* [pm] *vs. bond-angle* [°] *distortion vectors of the spiro* $C(C)_4$ *fragment in substituted spiro[4.4]-nonanes of type* **I**. ●: Structures with $s_2(E) > s_4(T_2)$, □: structures with $s_2(E) < s_4(T_2)$ (*cf. Fig. 3*). *a*) s_1 (A_1) *vs.* $s_2(E)$; linear regression: $s_1(A_1)$[pm] = −0.000872 (±0.001284) $s_2(E)$ + 0.01870 (±0.01769), $R = 0.116$. *b*) $s_3(T_2)$ *vs.* $s_2(E)$; linear regression: $s_3(T_2) = -0.00275$ (±0.000895) $s_2(E) + 0.02911$ (±0.01233), $T = 0.0529$.

$s_{2b}(E)$, and the bond-distance deformations $s_1(A_1)$ and $s_3(T_2)$[6]). Similarly, the $s_2(E)$ and $s_3(T_2)$ symmetry-deformation vectors are uncorrelated[7]) *(Fig. 5b)*.

In view of the large spread in both $s_2(E)$ and $s_3(T_2)$, the molecular dimensions for the central $C(C)_4$ fragments have been examined statistically [19]. For the 14 molecules, for which experimental standard deviations are available, the unweighted means ($\bar{x}_u$) and sample variances σ^2(sample) for bond angles and bond distances have been calculated and compared with averaged variances $\langle\sigma^2(x_i)\rangle$ by means of a χ^2 test. They are $\bar{x}_u = 109.50°$ with $\sigma(\bar{x}_u) = 1.28°$, $\sigma^2(\text{sample}) = 37.82$, $\langle\sigma^2(x_i)\rangle = 0.2123$, and $\chi^2 = 114827$ for bond angles, and $\bar{x}_u = 1.540$ Å with $\sigma(\bar{x}_u) = 0.004$ Å, $\sigma^2(\text{sample}) = 0.0004$, $\langle\sigma^2(x_i)\rangle = 0.00006$, and $\chi^2 = 2468$ for bond lengths. The values of χ^2 indicate that the variance in bond angles and distances is probably due to substitution effects, even though the quantities are uncorrelated.

Planarizing bond-angle distortions ($s_2(E)$) in the range of 20° *(cf. Fig. 5)* are thus virtually independent of bond-distance deformations ($s_1(A_1)$ and $s_3(T_2)$).

Conclusions. – Symmetry-deformation vectors have been used for a systematic analysis of planoid configurations of the spiro centre in polycyclic molecules containing spiro[4.4]nonane substructures with either no bridge between the two spiro rings or only bridges between the α,β'- or β,β'-positions. For evaluation of planoid distortions, the planarization index P_C is proposed.

The $s_{2a}(E)$ bond-angle distortions are all smaller than 0°. This is a consequence of the five-membered spiro rings, in which the average bond angle must be equal to or smaller than 108°. It is apparent from *Fig. 4* that the s_{2a}-type distortion is relatively constant, with an average value of $-12.5°\pm2.5°$, whereas the $s_{2b}(E)$ vector varies between 0° and 10°. In [10], spiro[4.4]nonanes with methylene chains bridging the α,α'-positions, including the fenestranes, will be discussed together with some energetic implications of distortion.

Appendix 1. – *Symmetry-Deformation Coordinates* S_1–S_5 [10]. Since only five of the six bond angles are geometrically independent, one of the six angular symmetry coordinates is redundant [12]. The symmetry deformation vectors are $s_{2a}(E) = s_{2a}S_{2a}(E)$, *etc.*, but $s_1(A_1) = (r_1 + r_2 + r_3 + r_4 - 4r_o)/2$, where r_o is a standard C–C bond length[6]).

$$S_1(A_1) = (r_1 + r_2 + r_3 + r_4)/2$$
$$S_{2a}(E) = (2\theta_{12} - \theta_{13} - \theta_{14} - \theta_{23} - \theta_{24} + 2\theta_{34})/\sqrt{12}$$
$$S_{2b}(E) = (\theta_{13} - \theta_{14} - \theta_{23} + \theta_{24})/2$$
$$S_{3a}(T_2) = (r_1 + r_2 - r_3 - r_4)/2$$
$$S_{3b}(T_2) = (r_1 - r_2 + r_3 - r_4)/2$$
$$S_{3c}(T_2) = (r_1 - r_2 - r_3 + r_4)/2$$
$$S_{4a}(T_2) = (\theta_{12} - \theta_{34})/\sqrt{2}$$
$$S_{4b}(T_2) = (\theta_{13} - \theta_{24})/\sqrt{2}$$
$$S_{4c}(T_2) = (\theta_{14} - \theta_{23})/\sqrt{2}$$
$$S_5(A_1) = (\theta_{12} + \theta_{13} + \theta_{14} + \theta_{23} + \theta_{24} + \theta_{34} - 6\theta_0)/\sqrt{6}$$

---

[6]) For a C–C bond, a standard bond length of 1.541 ± 0.003 Å has been used. Where C-atoms of the $C(C)_4$ fragment are part of a C=C of C=O bond, a value or $r_o = 1.53 \pm 0.01$ Å or 1.516 ± 0.005 Å, respectively, was used as standard [18].

[7]) The bond-angle and bond-length deformation vectors, $s_4(T_2)$ and $s_3(T_3)$, respectively, are uncorrelated as well (linear regression: $s_3(T_2)$[pm] = 0.000090 (±0.000417), $s_4(T_2)$[°] = +0.0247 (±0.0040), $R = 0.037$).

Appendix 2. – *Identification of Structures Analyzed.* The structures are listed according to their *CAS*-registry numbers, *Cambridge Datafile* identifiers, $s_{2a}(E)$, $s_{2b}(E)$, and $s_4(T_2)$ deformation vectors.

[21932-23-0] SNONDO (**1**) −9.988, 1.30, 1.556; [32603-30-8] BHMSIN (**2**) −14.145, 3.50, 2.236; [51768-54-8] DHGIBA (**3**) −11.374, 0.70, 5.679; [62182-25-6] HPSGIB (**4**) −11.576, 6.95, 5.529; [80455-68-1] BIKMOX (**5**) −12.940, 3.841, 5.379; [56587-28-1] SCBZFD (**6**) −20.727, 0.2, 7.913; [37558-43-3] SPINDO (**7**) −9.708, 0.675, 0.187; [60389-85-7] MCUNDB (**8**) −12.471, 9.10, 5.454; [75412-73-6] MOMAZL (**9**) −7.246, 1.35, 15.514; [79076-85-0] BAGBAM −14.087, 0.10. 5.253; [19124-90-4] GIBBME −11.114, 1.65, 7.117; [22882-63-9] GIBTME −11.893, 0.40, 6.771; [87038-77-5] BUHGUG −11.893, 6.60, 5.948; [79875-85-7] BAVBUV −12.298, 5.00, 6.313; [77-06-5] BUWZAU −10.852, 1.45, 7.501; [65342-61-2] HMMAZO −13.654, 2.35, 6.352; [60561-26-4] MAESCI −13.943, 0.250, 3.576; [159-66-0] BIPHME −14.751, 1.35, 1.7692; [72861-13-3] HMSIXZ −15.127, 1.70, 5.932; [58343-30-9] HMSPIN −14.145, 3.20, 0.283; [70223-78-8] HPMAZP −13.799, 4.20, 6.598; [76899-25-7] MBZAZL −10.652, 0.05, 4.859; [87448-39-3] CESBUX −13.943, 5.15, 4.107; [80161-71-3] LYCTON −12.124, 6.80, 8.684; [86699-53-8] BUJMEY −12.286, 5.714, 10.796; [62486-69-5] BEPDOP −11.501, 3.88, 8.479; [83329-74-2] BEVNUL −10.086, 7.59, 7.234; [81398-21-2] BIHXAR −13.293, 3.93, 4.243; [82854-15-7] BOGBOO −10.810, 1.88, 7.083; [85354-61-1] BOGCIJ −10.419, 3.03, 7.020; [82918-59-0] BOSNIG −15.401, 7.39, 19.673; [82918-60-3] BOSNOM −15.077, 7.53, 20.065; [82918-62-5] BOSNUS −12.796, 8.24, 21.269; [82950-40-1] BOSPAA −15.605, 7.02, 17.618; [8522-21-5] BUWVEU −18.044, 0.66, 7.881; [74585-68-5] DPIBFA −9.880, 5.27, 20.01.

This work was supported by the *Swiss National Science Foundation* (project No. 2.421-0.82 and 2.236-0.84).

REFERENCES

[1] J.H. van't Hoff, Voorstel tot uitbreiding der tegenwoordig in de scheikunde gebruikte strukturformules in de ruimte, Utrecht, 1874, *cf.* O. Krätz, *Chemie in unserer Zeit* **1974,** *8,* 135.
[2] J.A. Le Bel, *Bull. Soc. Chim. Fr.* **1874,** *22,* 337; *cf.* J. Weyer, *Chemie in unserer Zeit* **1974,** *8,* 143.
[3] a) K. Mislow, J. Siegel, *J. Am. Chem. Soc.* **1984,** *106,* 3319; b) R. Robinson, *Tetrahedron* **1974,** *30,* 1477.
[4] A. v. Baeyer, *Ber. Dtsch. Chem. Ges.* **1885,** *18,* 2277.
[5] A. Greenberg, J.F. Liebman, 'Strained Organic Molecules', 'Organic Chemistry', A Series of Monographs, Academic Press, New York, 1978, Vol. 38.
[6] P.E. Eaton, T.W. Cole, *J. Am. Chem. Soc.* **1964,** *86,* 3157.
[7] L.A. Paquette, R.J. Ternansky, D.W. Balogh, G. Kentgen, *J. Am. Chem. Soc.* **1983,** *105,* 5446.
[8] K.B. Wiberg, *Acc. Chem. Res.* **1984,** *17,* 379.
[9] P.E. Eaton, B.D. Leipzig, *J. Am. Chem. Soc.* **1983,** *105,* 1656.
[10] W. Luef, R. Keese, *Helv. Chim. Acta* **1987,** *70,* 543.
[11] P. Gund, T.M. Gund, *J. Am. Chem. Soc.* **1981,** *103,* 4458.
[12] a) P. Murray-Rust, H.B. Bürgi, J.D. Dunitz, *Acta Crystallogr.* **1978,** *34,* 1787; b) *ibid.* **1978,** *34,* 1793.
[13] W. Luef, R. Keese, unpublished results.
[14] M.J.S. Dewar, W. Thiel, *J. Am. Chem. Soc.* **1977,** *99,* 4899; QCPE No. 353.
[15] C. Altona, R.A.G. de Graaff, C.H. Leewestein, C. Romers, *J. Chem. Soc., Chem. Commun.* **1977,** 1305.
[16] M. Shiro, S. Hagishita, K. Kuriyama, *J. Chem. Soc., Perkin Trans. 2* **1976,** 1447.
[17] F.H. Allen, S. Bellard, M.D. Brice, B.A. Carthwright, A. Doublenday, H. Higgs, T. Hummelink, B.G. Peters, O. Kennard, W.D.S. Motherwell, J.R. Rodgers, D.G. Watson, *Acta Crystallogr., Sect. B* **1979,** *35,* 2331.
[18] R.C. Weast, 'Handbook of Chemistry and Physis', 59th edn., CRC Press, Inc., Florida, 1979, F-215.
[19] R. Taylor, O. Kennard, *Acta Crystallogr., Sect. B* **1983,** *39,* 517.